Pathological Findings of Saccular Cerebral Aneurysms - Impact of Subintimal Fibrin Deposition on Aneurysm Rupture -

Masaaki Hokari, MD, PhD; Naoki Nakayama, MD, PhD; Hiroshi Nishihara*, MD, PhD; Kiyohiro Houkin, MD, PhD

Department of Neurosurgery and Pathology*, Hokkaido University Graduate School of Medicine

Correspondence:

Masaaki Hokari, MD, PhD,

Department of Neurosurgery, Hokkaido University Graduate School of Medicine, North 15 West 7, Kita-ku, Sapporo 060-8638, Japan

TEL : +81-11-706-5987 FAX : +81-11-708-7737

E-mail: karimasa@med.hokudai.ac.jp

Abstract

Although several studies have suggested that aneurysmal wall inflammation and laminar thrombus are associated with the rupture of saccular aneurysms, the mechanisms leading to the rupture remain obscure. We performed full exposure of aneurysms before clip application and attempted to keep the fibrin cap on the rupture point. Using these specimens in a nearly original state before surgery, we conducted a pathological analysis and studied the differences between ruptured and unruptured aneurysms to clarify the mechanism of aneurysmal wall degeneration. This study included ruptured (n=28) and unruptured (n=12) saccular aneurysms resected after clipping. All of the ruptured aneurysms were obtained within 24 hours of onset. Immunostainings for markers of inflammatory cells (CD68) and classical histological staining techniques were performed. Clinical variables and pathological findings from ruptured and unruptured aneurysms were compared. Patients with ruptured or unruptured aneurysms did not differ by age, gender, size, location, and risk factors, such as hypertension, smoking, and hyperlipidemia. The absence or fragmentation of the internal elastica lamina, the myointimal hyperplasia, and the thinning of the aneurysmal wall were generally observed in both aneurysms. The existence of subintimal fibrin deposition, organized laminar thrombus, intramural hemorrhage, neovascularization and monocyte infiltration are more frequently observed in ruptured aneurysms. Multivariate logistic regression analysis showed that ruptured aneurysm was associated with presence of subintimal fibrin deposition and monocyte infiltration. These findings suggest that subintimal fibrin deposition and chronic inflammation have a strong impact on degeneration of the aneurysmal wall leading to their rupture, and this finding may be caused by endothelial dysfunction.

Keywords: aneurysms; pathology; endothelial dysfunction

Introduction

Despite modern therapy, the mortality of subarachnoid hemorrhage is still high especially in poor grade patients [16, 17, 30]. Thus, recent progress in noninvasive imaging techniques has resulted in increased detection of unruptured aneurysms and many surgical interventions have been performed to prevent future ruptures [1, 11]. In contrast, there are recommendations against interventions for unruptured aneurysms because of the relatively low risk of rupture [3, 29]. There is an additional issue, namely, the discrepancy between the low rupture rate of small unruptured aneurysms and the sizes of ruptured aneurysm[33]. According to previous reports [29, 38], the rupture rate is not constant after formation and may be higher in the early stages. Ruptured aneurysms, therefore, may be fundamentally different from stable aneurysms that have remained unruptured for several years. Although it is clear that we should only perform interventions for unruptured aneurysms with a high risk of rupture, predicting aneurysmal ruptures have not been promising at present.

To clarify the mechanisms leading to their rupture, the number of pathological examinations for cerebral aneurysms is increasing [2, 4-6, 15, 24, 25, 35]. Previous animal experiments indicated that aneurysmal formation and enlargement were strongly associated with chronic inflammation mainly caused by T-lymphocytes and macrophages [2, 24]. Moreover, several studies on human saccular aneurysms have contributed to the notion that chronic inflammation plays a role in aneurysmal wall degeneration and potentially increases subsequent risk of rupture [4, 6, 7, 15, 35]. In human aneurysms, Hasan et al. reported that frequent use of aspirin could conceivably play a role in reducing the risk of aneurysmal progression to rupture [9]. They speculated that aspirin has inhibitory effects on several inflammatory mediators postulated to play a role in cerebral aneurysm pathology. Furthermore, according to another report [25], the aneurysmal wall is prone to

thrombosis in the lining of the luminal wall because of altered flow conditions. Frosen et al. reported in their pathological examinations that luminal thrombosis as well as chronic inflammation in the ruptured aneurysm wall was observed at higher incidence than in the unruptured wall [6, 7]. Thus, several previous pathological studies have suggested that aneurysmal wall inflammation and laminar thrombosis were associated with ruptured aneurysms. The mechanisms leading to their rupture, however, still remained obscure.

Currently, the authors usually perform full exposure of aneurysms before clip application and attempted to keep the fibrin cap on the rupture point, and then perform neck clippings. After resection, aneurysmal specimens in a nearly original state before surgery can be obtained. Using these specimens, we performed a pathological analysis of aneurysms and studied the differences between ruptured and unruptured aneurysms to clarify the mechanism of aneurysmal wall degeneration.

Patients and Methods

Patients

This study included ruptured (n=28) and unruptured (n=12) saccular aneurysms resected after microsurgical clipping, from years 2007-2011 (Table 1). All of the ruptured aneurysms in this study were obtained within 24 hours from onset. To obtain specimens of saccular ruptured and unruptured aneurysms in a nearly original state before surgery, we performed full exposure of the aneurysms before clip application, attempted to keep the fibrin cap on the rupture point, and then performed neck clippings as shown in Fig. 1A-B (Case 18). After the environment for clip

insertion (which may be tentative) and a temporary occlusion of the parent artery was obtained, the outside surface of the cap of the hemostatic fibrin clot on the ruptured point was detached gradually and carefully from adjacent structures. After confirming safety, we resected them (Fig. 1C-D). However, this method is not always possible in all cases. We did not resect the aneurysm sac when full exposure was considered too dangerous during surgery. Therefore, we excluded most of those aneurysms, such as small aneurysms, aneurysms with a rupture point near the neck, or aneurysms with a very thick neck because the resection of the aneurysmal sac would be dangerous. Thus, we obtained a total of 40 specimens of aneurysms during the study period.

Clinical data were collected from the patients' medical records. Aneurysmal locations were classified as follows: (1) internal carotid artery aneurysm (ICA); (2) middle cerebral artery aneurysm (MCA); and (3) anterior cerebral artery aneurysm (ACA) including anterior communicating artery and distal ACA aneurysms. Sizes of aneurysms were measured from preoperative vascular imaging studies, either three-dimensional computed tomographic angiography (3D-CTA) or digital subtraction angiography (DSA). This study was approved by the ethics committee of Hokkaido University.

Histology and Immunohistochemistry

After aneurysm resection, specimens were gently washed out with saline to remove any blood and then fixed in 10% formalin. For classical histological stainings, sections were stained with hematoxykin-eosin (HE) and Elastica-Masson (EM) methods. We also performed phospho tungstic acid hematoxylin (PTAH) stainings to detect and confirm fibrin components of the specimens. PTAH staining was originally established by Mallory for glial fiber staining, but now it is also used for the demonstration of fibrin [8, 12, 22, 23, 26]. Although the mechanism of the staining reaction

obtained by PTAH is largely unknown, PTAH stains the collagen pink, glial fibers, muscle fibers, and fibrin blue [22, 23, 26]. As for immunohistochemistry, we used CD68 as a marker of macrophage infiltration. The deparaffinized sections were processed through antigen retrieve for 15 min, and then were incubated with primary mouse monoclonal antibody against human CD68 (Dako, 1:100). Then, the immunoreactivity was visualized by treating with Dako Envision kit HRP (DAB) (Dako). Finally, sections were counterstained with hematoxylin.

Histological analysis

By observing HE and EM sections through an optical microscope (Olympus BX50), we evaluated pathological variables such as the absence or fragmentation of the internal elastica lamina, myointimal hyperplasia (>200μm), thinning of aneurysmal wall (<50μm), intramural hemorrhage, and neovascularization in the aneurysmal wall. The existence of subintimal fibrin deposition was evaluated by PTAH and HE stainings. There was a hyaline-like structure under the intimal layer in HE sections, which was also identified in PTAH sections a deeply blue-stained layer. The number of CD68 positive cells in an area (100 μm×100 μm) of the aneurysmal wall where the active invasion of inflammatory cells was observed on HE was determined by counting under ×40 magnification. The severe prevalence of infiltration by chronic inflammatory cells infiltration is defined as having more than fifty CD68 positive cells in the area; mild infiltration is defined as having more than ten CD68 positive cells.

Statistics

All data are expressed as mean ± SD. Clinical variables, including age, gender, aneurysm size,

location, multiple aneurysms, history of hypertension, smoking, history of hyperlipidemia, and intake of statins and pathological variables between ruptured and unruptured aneurysms were compared by use of χ^2 test or unpaired t-test, as appropriate. Multivariate logistic regression analysis was performed to determine whether ruptured aneurysm was associated with the clinical variables with a P value of <0.1 in univariate analysis. Differences with a P value of <0.05 were considered statistically significant.

Results

Clinical Data and Radiological Findings

"Characteristics of the patients in this study are shown in Table 2. The participants were composed of 17 men and 23 women. The mean age of total patients was 63.1±9.5 years-old, and mean size of aneurysms was 6.9±3.8 mm. The ratio of the women, the incidence of history of hypertension and smoking were slightly higher in the ruptured group than in the unruptured group, and history of hyperlipidemia and intake of statins were more frequently observed in the ruptured group than in the unruptured (46.4% and 17.9% in the ruptured versus 25% and 8.3% in the unruptured, respectively). There were also no differences in aneurysm characteristics such as location and size, which may have been caused by our judgment to be safe in full exposure and aneurysmal sac resection. Across all clinical and radiological data, there were no statistically significant differences.

Histology of cerebral saccular aneurysms

Representative photos of the unruptured and ruptured aneurysms are shown in Fig.2 and Figs. 3-6. As shown in Fig. 2 (unruptured aneurysm of Case 35), the thickness of the aneurysmal wall was varied and the areas where it had thinned significantly were generally observed in all cases, even in unruptured aneurysms (Fig. 2B). At the thickened part of wall (Fig. 2C), the outer membrane (red arrow), the degenerated media (dotted arrow), the fragmental internal elastica lamina (triangle) and the intima (black arrow) were observed. In an atherosclerotic cerebral artery (Fig. 2E), the outer membrane (red arrow), the media (dotted arrow), the internal elastica lamina (triangle) and the thickened intima (black arrow) were also clearly observed. However, in the area where the wall transitions from thick to thin (Fig.2D), the thinning part was composed of only the outer membrane (red arrow), while the media (dotted arrow) and the intima (black arrow) were absent. In this case, the thickness of the thinned part of wall was measured to be approximately 20 μm. Similar findings were also observed in most of the other unruptured aneurysms.

In the ruptured case presented in Fig. 3 (Case 1), the aneurysmal wall was interrupted at the rupture point (triangles in Fig. 3B). Near the rupture point (Fig. 3C), we observed a hyaline-like lined structure under the intimal layer on the HE sections (left panel of Fig. 3C), which was identified on PTAH sections as a deeply blue-stained layer (center panel of Fig. 3C). There were no erythrocytes in this layer. CD68 positive cells were also identified in this area (right panel of Fig. 3C). Thus, we determined that fibrin components and the infiltration of chronic inflammatory cells were present before the rupture of aneurysm.

Furthermore, even in parts of the wall far from the rupture point (Fig. 3D), similar pathological findings such as subintimal fibrin deposition, and infiltration of CD68 positive cells were observed. In the ruptured aneurysm described in Case 18 (in Fig. 1and Fig. 4), a thinned aneurysmal wall and subintimal fibrin deposition were clearly observed (arrows in Fig. 4A). There were numerous CD68 positive cells, especially in the area near the rupture point (Fig. 4B-D), which also suggested

the presence of chronic inflammation prior to the rupture. Additionally, as shown in Fig. 5 (Case 7), severe infiltration of inflammatory cells was found in the aneurysmal wall (arrows in Fig. 5A-B) far from the rupture point (arrow heads in Fig. 5A-B). The numerous inflammatory cells had round nuclei and CD68 positive cells, indicating that they are mainly lymphocytes and macrophages (Fig. 5C-D).

Interestingly, another ruptured aneurysm (Case 15) had organized laminar thrombus at the aneurysmal wall (arrows in Fig. 6A-B and 6C-D) far from the rupture point (arrow heads in Fig. 6A-B). Neovascularization and chronic inflammation in the wall were also observed in the layer of organized laminar thrombus (Fig. 6C-D). Thus, concurrent findings such as subintimal fibrin deposition, organized laminar thrombus, intramural hemorrhage, neovascularization in the wall, and monocyte infiltration were frequently observed in most of the ruptured aneurysms not only at the rupture point, but also in unruptured areas.

Factors Associated with Rupture

A summary of the pathological findings of this study is presented in Table 2. The absence or fragmentation of internal elastica lamina, myointimal hyperplasia, and thinning of the aneurysmal wall were generally observed in both ruptured and unruptured aneurysms. The existence of organized laminar thrombus was more frequently observed in the ruptured group than in the unruptured group, although this difference is not statically significant. The presence of subintimal fibrin deposition, intramural hemorrhage, and neovascularization in the wall were more frequently observed in the ruptured group than in the unruptured group, with significance determined according to univariate analysis using χ^2 test. The number of CD68-positive cells was 70.2 ± 29.5 in the ruptured group. However, the values were 8.6 ± 17.6 in the unruptured group. Thus, the number

of CD68-positive cells in the aneurysmal wall was significantly smaller in the unruptured group than in the ruptured group (P <0.001). Monocyte infiltration (total or severe) was more frequently observed in the ruptured group than in the unruptured group, with significance determined according to univariate analysis using χ^2 test. Using these variables with a P value of <0.1 in univariate analysis, multivariate logistic regression analysis showed that the ruptured aneurysm was associated with the existence of subintimal fibrin deposition (p=0.015) and severe monocyte infiltration (p=0.019).

Discussion

In this study, subintimal fibrin deposition containing no erythrocytes was detected in most of the ruptured aneurysms resected within 24 hours of onset. This indicates that the fibrin components in the subintimal layer were present prior to rupture. Moreover, this study confirmed that ruptured aneurysms are closely associated with the existence of subintimal fibrin deposition. Although subintimal fibrin deposition was reported in microaneurysms of patients with amyloid angiopathy [19], we are not aware of any published reports concerning subintimal fibrin deposition in cerebral saccular aneurysms.

Instead, what Frosen et al. described as an 'extremely thin thrombosis-lined hypocellular wall' in their figure (Figure 1D of their article)[6] essentially resembles what we call subintimal fibrin deposition. Moreover, Kataoka et al found that degenerated walls with hyaline deposits mostly ruptured:[15] the hyaline deposits referred to in their report may be the same as our findings. As the figures in both Kataoka et al. and our reports demonstrate, the pathological findings that indicate hyaline deposits or fibrinoid necrosis correspond to the lined structure of fibrin components beneath

the endothelial cells. Although they may indicate that the thin lining of luminal thrombosis are covered with endothelial cells in the course of organization, we conjectured that blood plasma passing through the tight junction of endothelial cells causes fibrin components to be deposited into the subintimal layer. Thus, we determined that the observations could be caused by continuous endothelial dysfunction.

Indeed, several investigators reported that endothelial dysfunction is associated with cerebral aneurysm formation or aneurysmal rupture [7, 15, 34]. By using scanning electron microscopy (SEM), Kataoka et al. found that endothelial cell arrangement was damaged or disrupted in most ruptured aneurysms, whereas the inner surface of the aneurysmal sac was completely covered with normally- shaped endothelial cells in unruptured aneurysms [15]. In this study, however, an endothelial evaluation was not conducted because additional treatment was required to perform the investigations for SEM immediately following resection. Therefore, it was impossible to directly compare the findings of subintimal fibrin deposition with tight junction disorder confirmed by SEM. In order to clarify the mechanism of aneurysmal wall degeneration associated with endothelial functions, a step by step process is required. Thus, further investigations should be performed to ensure endothelial placements and tight junction by electronic microscopy to prove endothelial dysfunction.

Our study also demonstrated that the existence of organized laminar thrombus, intramural hemorrhage, neovascularization in the wall and monocyte infiltration were more frequently observed in the ruptured group, despite the lack of statistical significance. As shown in Fig. 6, organized laminar thrombosis and neovascularization in the wall were occasionally observed at unruptured sites of ruptured aneurysms. These current findings may agree with those from previous studies, indicating that thrombi easily from and remained attached to a dysfunctional endothelial vessel wall [6]. These findings suggest that, in the wall with laminar thrombosis, circulating inflammatory

cells invade the thrombus. This inflammatory response and hypoxia of intima attributable to laminar thrombosis promote neovascularization in the wall [14].

The existence of a laminar thrombus and thrombus in the aneurysm has been regarded as a risk factor of rupture in the dissecting, fusiform, or giant saccular aneurysms [18, 20, 21, 27, 28]. Although most of the patients in this study had non-giant aneurysms and there were no thrombosed aneurysms confirmed by pre-operative radiological examination and intraoperative findings, some had laminar thrombus confirmed by pathological examination. Furthermore, fibrin deposition, chronic inflammation, and laminar thrombosis were observed even in sections of the wall far from the rupture point, as our figures demonstrate. This finding is quite as it may indicate that wall degeneration can likely be attributed to dysfunction of endothelial cells occurring simultaneously in different portions of the ruptured aneurysms.

The absence or fragmentation of the internal elastica lamina and the thinning of the aneurysmal wall are generally observed in unruptured aneurysms, but organized laminar thrombus, subintimal fibrin deposition, intramural hemorrhage, and neovascularization in the wall are rarely detected. In this study, monocyte infiltration was found in four of 12 unruptured aneurysms, but severe invasion was found in only one instance. In our study, therefore, multivariate logistic regression analysis showed that ruptured aneurysms were associated with the existence of severe monocyte infiltration, and the number of CD68-positive cells in the aneurysmal wall was significantly smaller in the unruptured group than in the ruptured group. In contrast to this result, however, previous animal studies in unruptured aneurysms have suggested that aneurysmal formation and enlargement are strongly associated with chronic inflammation [2, 24]. Hence, there is a question regarding the discrepancy between inflammatory findings of the unruptured aneurysms in our study and previous reports.

According to previous clinical reports [13, 36], most unruptured aneurysms in humans identified through routine clinical tests are stable in size, whereas the aneurysms in animal models are prone to

enlarge rapidly. This may be one of the reasons for this discrepancy. In addition, although the pathological report from Chyatte et al. emphasized chronic inflammation in both ruptured and unruptured aneurysms [4], the results of our current study concur with those of Frosen et al., which concluded that inflammatory findings in the unruptured aneurysms wall were not severe [6]. This suggests that there are a small number of inflammatory cells in most types of unruptured aneurysms, i.e. asymptomatic and non-growing aneurysms, excepting those that are symptomatic or rapidly growing.

In regards to clinical prediction of rupture, MRI and computational flow dynamics (CFD) may be useful in detecting these tiny laminar thrombus formations and chronic inflammation in the wall. Hasan et al. recently reported a unique pilot study about macrophage imaging within human aneurysm walls using ferumoxyol-enhanced MRI [10], and its clinical use should be expected in the future. Finally, several recent reports suggested that CFD can analyze complex hemodynamics in the aneurysms and evaluate the dangerous hemodynamic state leading to rupture [31, 32, 37]. Although CFD cannot directly detect thrombus or inflammation, this clinical tool may evaluate the site where endothelial cells would be easily injured by analyzing hemodynamics like wall shear stress (WSS) and turbulence [32]. In the future, predicting risk for rupture may be possible if pathological findings are compared with results from noninvasive imaging tools such as MRI and CFD.

Conclusions

We confirmed that a ruptured aneurysm is closely associated with the existence of severe monocyte infiltration and subintimal fibrin deposition, and we speculated that blood plasma passed through the

tight junction of endothelial cells and fibrin components were deposited in the subintimal layer. Further investigation is needed to confirm endothelial function via using electronic microscopy and comparing pathological observations with radiological findings.

Acknowledgements

The authors thank Yumiko Shinohe deeply for her technical assistance. This study was supported by Grant-in-aid from the Ministry of Education, Science and Culture of Japan (No.011-0321).

References

1. Akiyama Y, Houkin K, Nozaki K, Hashimoto N Practical decision-making in the treatment of unruptured cerebral aneurysm in Japan: the U-CARE study. Cerebrovasc Dis 30:491-499

2. Aoki T, Kataoka H, Ishibashi R, Nozaki K, Hashimoto N (2008) Simvastatin suppresses the progression of experimentally induced cerebral aneurysms in rats. Stroke 39:1276-1285

3. Caplan LR (1998) Should intracranial aneurysms be treated before they rupture? N Engl J Med 339:1774-1775

4. Chyatte D, Bruno G, Desai S, Todor DR (1999) Inflammation and intracranial aneurysms. Neurosurgery 45:1137-1146; discussion 1146-1137

5. Frosen J, Marjamaa J, Myllarniemi M, Abo-Ramadan U, Tulamo R, Niemela M, Hernesniemi J, Jaaskelainen J (2006) Contribution of mural and bone marrow-derived neointimal cells to thrombus organization and wall remodeling in a microsurgical murine saccular aneurysm model. Neurosurgery 58:936-944; discussion 936-944

6. Frosen J, Piippo A, Paetau A, Kangasniemi M, Niemela M, Hernesniemi J, Jaaskelainen J (2004) Remodeling of saccular cerebral artery aneurysm wall is associated with rupture: histological analysis of 24 unruptured and 42 ruptured cases. Stroke 35:2287-2293

7. Frosen J, Tulamo R, Paetau A, Laaksamo E, Korja M, Laakso A, Niemela M, Hernesniemi J (2012) Saccular intracranial aneurysm: pathology and mechanisms. Acta Neuropathol 123:773-786

8. Halvorsen AM, Futrell N, Wang LC (1994) Fibrin content of carotid thrombi alters the production of embolic stroke in the rat. Stroke 25:1632-1636

9. Hasan DM, Mahaney KB, Brown RD, Jr., Meissner I, Piepgras DG, Huston J, Capuano AW, Torner JC (2011) Aspirin as a Promising Agent for Decreasing Incidence of Cerebral Aneurysm Rupture. Stroke 42:3156-3162

10. Hasan DM, Mahaney KB, Magnotta VA, Kung DK, Lawton MT, Hashimoto T, Winn HR, Saloner D, Martin A, Gahramanov S, Dosa E, Neuwelt E, Young WL (2012) Macrophage imaging within human cerebral aneurysms wall using ferumoxytol-enhanced MRI: a pilot study. Arterioscler Thromb Vasc Biol 32:1032-1038

11. Hokari M, Kuroda S, Nakayama N, Houkin K, Ishikawa T, Kamiyama H Long-term prognosis in patients with clipped unruptured cerebral aneurysms-increased cerebrovascular events in patients with surgically treated unruptured aneurysms. Neurosurg Rev

12. Huber A, Dorn A, Witzmann A, Cervos-Navarro J (1993) Microthrombi formation after severe head trauma. Int J Legal Med 106:152-155

13. Inoue T, Shimizu H, Fujimura M, Saito A, Tominaga T (2012) Annual rupture risk of growing unruptured cerebral aneurysms detected by magnetic resonance angiography. J Neurosurg 117:20-25

14. Kano Tsuneo, Hirayama Teruyasu, Katayama Yoichi (2003) Unruptured Thrombosed Giant Aneurysm: Strategy for Treament. Surg Cereb Stroke (Jpn) 31:344-348

15. Kataoka K, Taneda M, Asai T, Kinoshita A, Ito M, Kuroda R (1999) Structural fragility and inflammatory response of ruptured cerebral aneurysms. A comparative study between ruptured and unruptured cerebral aneurysms. Stroke 30:1396-1401

16. Kazumata K, Kamiyama H, Ishikawa T, Nakamura T, Takizawa K, Komeichi T, Kubota T, K T (2004) Current Surgical Outcome in Poor Grade Patients with Subarachnoid Hemorrhage. Surg Cereb Stroke (Jpn) 32:103-106

17. Kuroda S, Ishikawa T, Hokari M, Nakayama N, Yasuda H, Yoshimoto T, Ushikoshi S, Kazumata K, Itamoto Kouji, Asano Takeshi, Aoki Takeshi, Kobayashi Tohru, Takikawa Shugo, NIiya Yoshimasa, Takahashi Akihiro, Terasaka Shunsuke, Aida Toshimitsu, Mabubchi Shoji , Nomura Mikio, Saito Hisatoshi , Kaneko Sadao, Yoshinobu I (2009) Epidemiology,Therapy and Functional Outcome of Aneurysmal Subarachnoid Hemorrhage in Sapporo Between 2003-2007: An Area-specific, Group-based Study by Hokkaido University Hospital Group. Surg Cereb Stroke (Jpn) 37:109-115

18. Lawton MT, Quinones-Hinojosa A, Chang EF, Yu T (2005) Thrombotic intracranial aneurysms: classification scheme and management strategies in 68 patients. Neurosurgery 56:441-454; discussion 441-454

19. Maeda A, Yamada M, Itoh Y, Otomo E, Hayakawa M, Miyatake T (1993) Computer-assisted three-dimensional image analysis of cerebral amyloid angiopathy. Stroke 24:1857-1864

20. Martin AJ, Hetts SW, Dillon WP, Higashida RT, Halbach V, Dowd CF, Lawton MT, Saloner D (2011) MR imaging of partially thrombosed cerebral aneurysms: characteristics and evolution. AJNR Am J Neuroradiol 32:346-351

21. Mizutani T (1996) A fatal, chronically growing basilar artery: a new type of dissecting aneurysm. J Neurosurg 84:962-971

22. Moe N (1969) The deposits of fibrin and fibrin-like materials in the basal plate of the normal human placenta. Acta Pathol Microbiol Scand 75:1-17

23. Moe N, Abildgaard U (1969) Histological staining properties of in vitro formed fibrin clots and precipitated fibrinogen. Acta Pathol Microbiol Scand 76:61-73

24. Moriwaki T, Takagi Y, Sadamasa N, Aoki T, Nozaki K, Hashimoto N (2006) Impaired progression of cerebral aneurysms in interleukin-1beta-deficient mice. Stroke 37:900-905

25. Nussel F, Wegmuller H, Huber P (1993) Morphological and haemodynamic aspects of cerebral aneurysms. Acta Neurochir (Wien) 120:1-6

26. Pearse AG (1968) Histochemistry, 3rd ed. J.A. Churchill, London:642

27. Rayz VL, Boussel L, Ge L, Leach JR, Martin AJ, Lawton MT, McCulloch C, Saloner D (2010) Flow residence time and regions of intraluminal thrombus deposition in intracranial aneurysms. Ann Biomed Eng 38:3058-3069

28. Roccatagliata L, Guedin P, Condette-Auliac S, Gaillard S, Colas F, Boulin A, Wang A, Guieu S, Rodesch G (2010) Partially thrombosed intracranial aneurysms: symptoms, evolution, and therapeutic

management. Acta Neurochir (Wien) 152:2133-2142

29. Sato K, Yoshimoto Y (2011) Risk profile of intracranial aneurysms: rupture rate is not constant after formation. Stroke 42:3376-3381

30. Shim JH, Yoon SM, Bae HG, Yun IG, Shim JJ, Lee KS, Doh JW Which treatment modality is more injurious to the brain in patients with subarachnoid hemorrhage? Degree of brain damage assessed by serum S100 protein after aneurysm clipping or coiling. Cerebrovasc Dis 34:38-47

31. Shojima M, Nemoto S, Morita A, Oshima M, Watanabe E, Saito N (2010) Role of shear stress in the blister formation of cerebral aneurysms. Neurosurgery 67:1268-1274; discussion 1274-1265

32. Shojima M, Oshima M, Takagi K, Torii R, Hayakawa M, Katada K, Morita A, Kirino T (2004) Magnitude and role of wall shear stress on cerebral aneurysm: computational fluid dynamic study of 20 middle cerebral artery aneurysms. Stroke 35:2500-2505

33. Sonobe M, Yamazaki T, Yonekura M, Kikuchi H (2010) Small unruptured intracranial aneurysm verification study: SUAVe study, Japan. Stroke 41:1969-1977

34. Tada Y, Yagi K, Kitazato KT, Tamura T, Kinouchi T, Shimada K, Matsushita N, Nakajima N, Satomi J, Kageji T, Nagahiro S (2010) Reduction of endothelial tight junction proteins is related to cerebral aneurysm formation in rats. J Hypertens 28:1883-1891

35. Tulamo R, Frosen J, Junnikkala S, Paetau A, Kangasniemi M, Pelaez J, Hernesniemi J, Niemela M, Meri S (2010) Complement system becomes activated by the classical pathway in intracranial aneurysm walls. Lab Invest 90:168-179

36. Wermer MJH, van der Schaaf IC, Velthuis BK, Algra A, Buskens E, Rinkel GJE (2005) Follow-up screening after subarachnoid haemorrhage: frequency and determinants of new aneurysms and enlargement of existing aneurysms. Brain 128:2421-2429

37. Yamaguchi R, Ujiie H, Haida S, Nakazawa N, Hori T (2008) Velocity profile and wall shear stress of saccular aneurysms at the anterior communicating artery. Heart Vessels 23:60-66

38. Yonekura M (2004) Small unruptured aneurysm verification (SUAVe Study, Japan)--interim report. Neurol Med Chir (Tokyo) 44:213-214

FIGURE LEGENDS

Fig. 1

Intraoperative photographs of Case 18 (ruptured right middle cerebral artery aneurysm)

The aneurysm was fully exposed while keeping the fibrin cap on the rupture point before clip application (Fig. 1A) after which neck clipping was performed (Fig. 1B). Once we determined resection could be performed safety,, the aneurysm was resected (Fig. 1C-D).

Fig. 2

Intraoperative photograph (Fig. 2A) and representative photomicrographs of Elastica-Massson (EM) stained sections (Fig. 2B-D) of Case 35 (unruptured right middle cerebral artery aneurysm) and of a normal cerebral artery (Fig.2E). At the thickened part of wall (Fig. 2C), the outer membrane (red arrow),the degenerated media (dotted arrow), the fragmented internal elastica lamina (triangle) and the intima (black arrow) were observed. In an atherosclerotic cerebral artery (Fig. 2E), the outer membrane (red arrow), the media (dotted arrow), the internal elastica lamina (triangle) and the thickened intima (black arrow) were clearly observed. Scale bar in Fig. 2B; 200μm, in Fig. 2C and 2E; 50μm, and Fig. 2D; 20μm.

Fig. 3

Intraoperative photograph (Fig. 3A) and representative photomicrographs of Case 1 (ruptured left middle cerebral artery aneurysm); EM (Fig. 3B), HE (Left panel of Fig. 3C and 3D), PTAH (center panel of Fig. 3C and 3D), and CD68 (right panel of Fig. 3C and 3D). Scale bar in Fig.3B; 500μm, in left and center panel of Fig. 3C-D; 100μm, in right panel of Fig. 3C; 20μm, and in right panel of Fig. 3D; 50μm

Fig. 4

Representative photomicrographs of Case 35 (ruptured right middle cerebral artery aneurysm); EM (Fig. 4A) and CD68 (Fig. 4B-D): Fig.4C; upper square in Fig. 4B, Fig. 4D; lower square in Fig. 4B.

Scale bar in Fig. 4A-B; 200μm. Scale bar in Fig. 4C-D, 20μm.

Fig. 5

Intraoperative photograph (Fig. 5A) and representative photomicrographs of Case 7 (ruptured right middle cerebral artery aneurysm); EM (Fig. 5B), HE (Fig. 5C and left panel of Fig. 5D), and CD68 (right panel of Fig. 5D). Scale bar in Fig. 5B; 500μm, in Fig. 5C; 100μm, and in Fig. 5C; 20μm.

Fig. 6

Intraoperative photograph (Fig. 6A) and representative photomicrographs of Case 15 (ruptured anterior communicating artery aneurysm); EM (Fig. 6B), HE (Fig. 6C), and CD68 (Fig. 6D). Scale bar in Fig. 6B; 500μm, and in Fig. 6C-D; 100μm.

Fig. 1

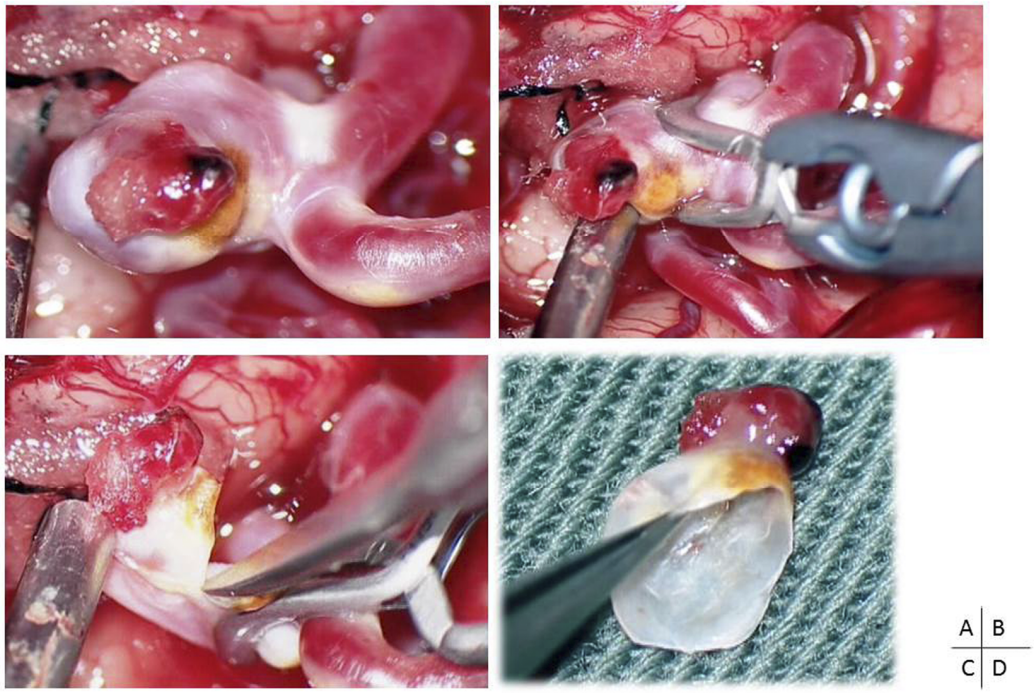

Fig. 2

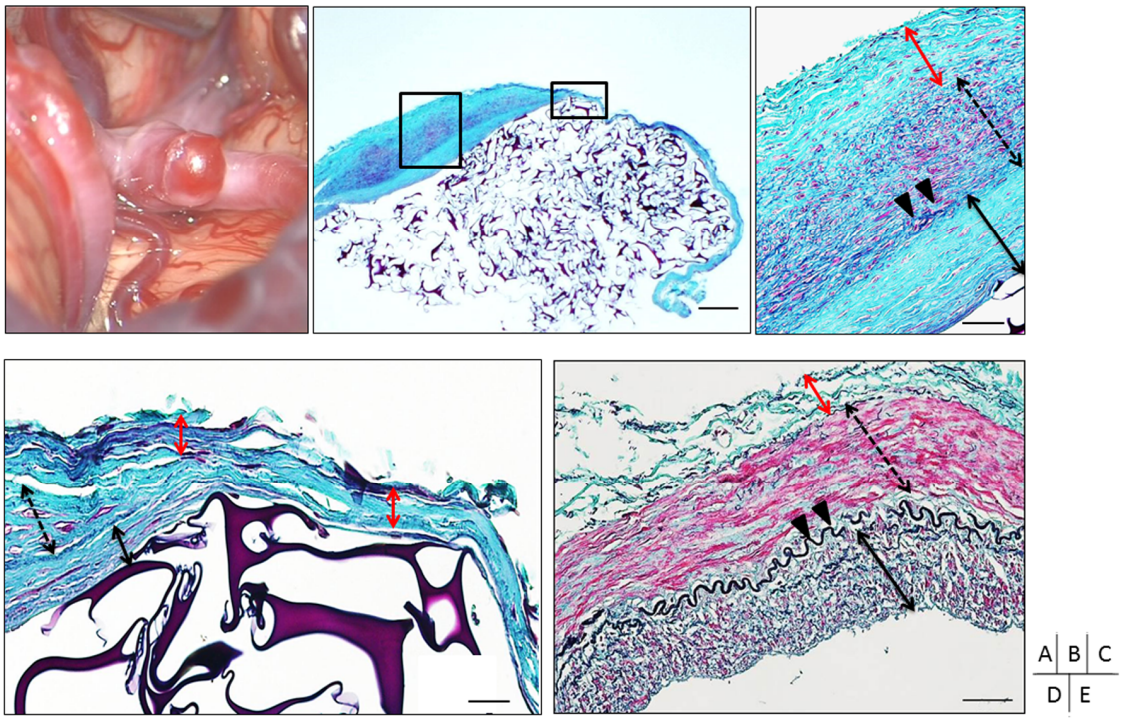

Fig. 3

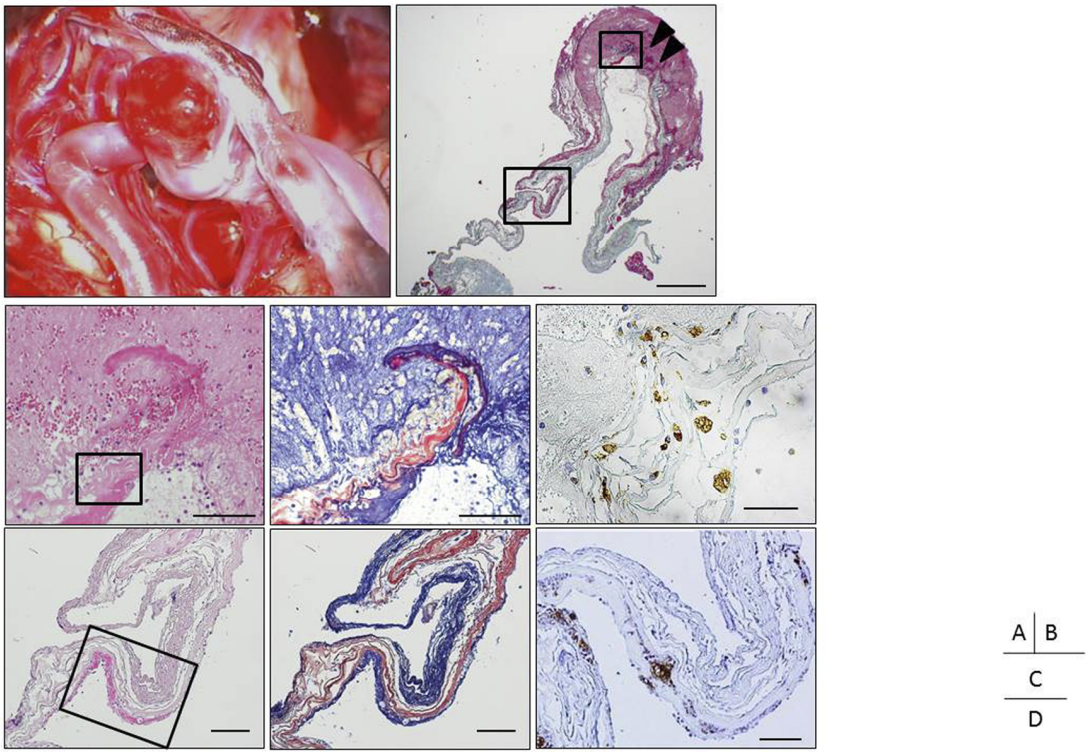

Fig. 4

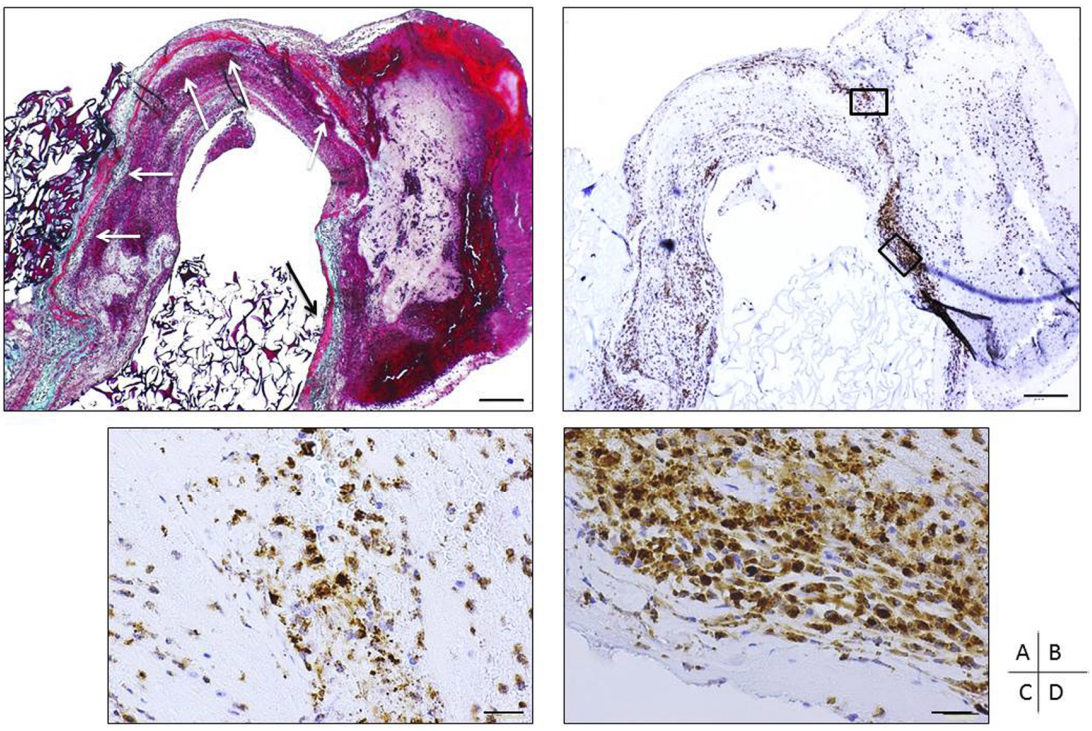

Fig. 5

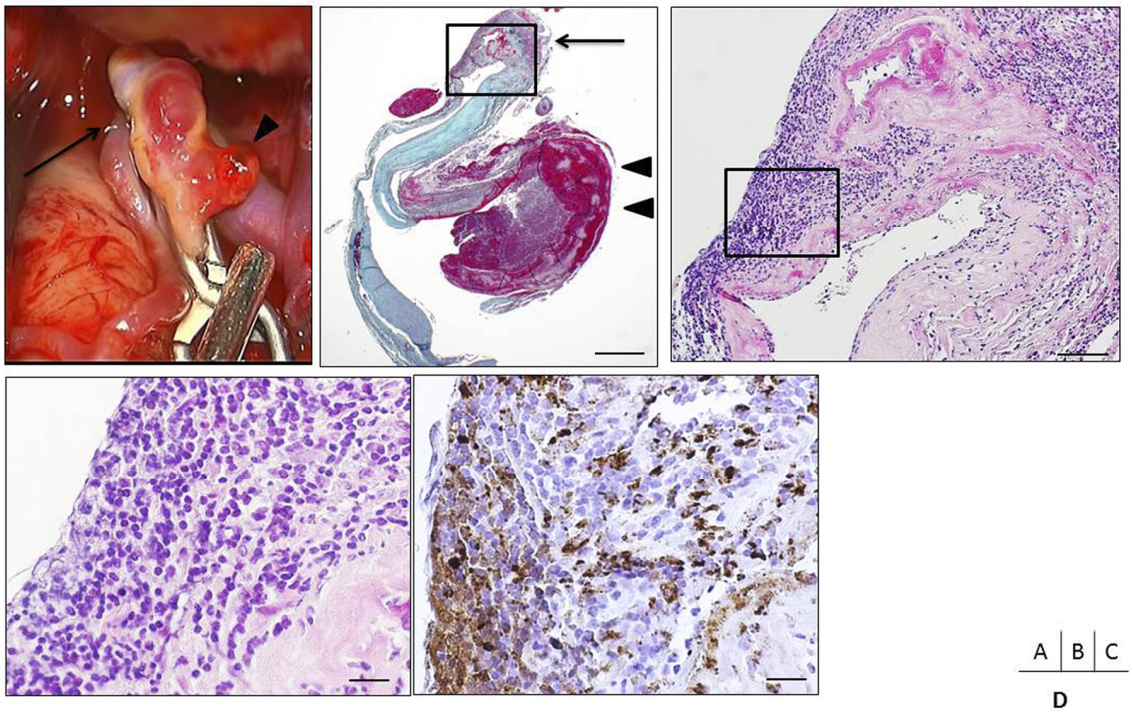

Fig. 6

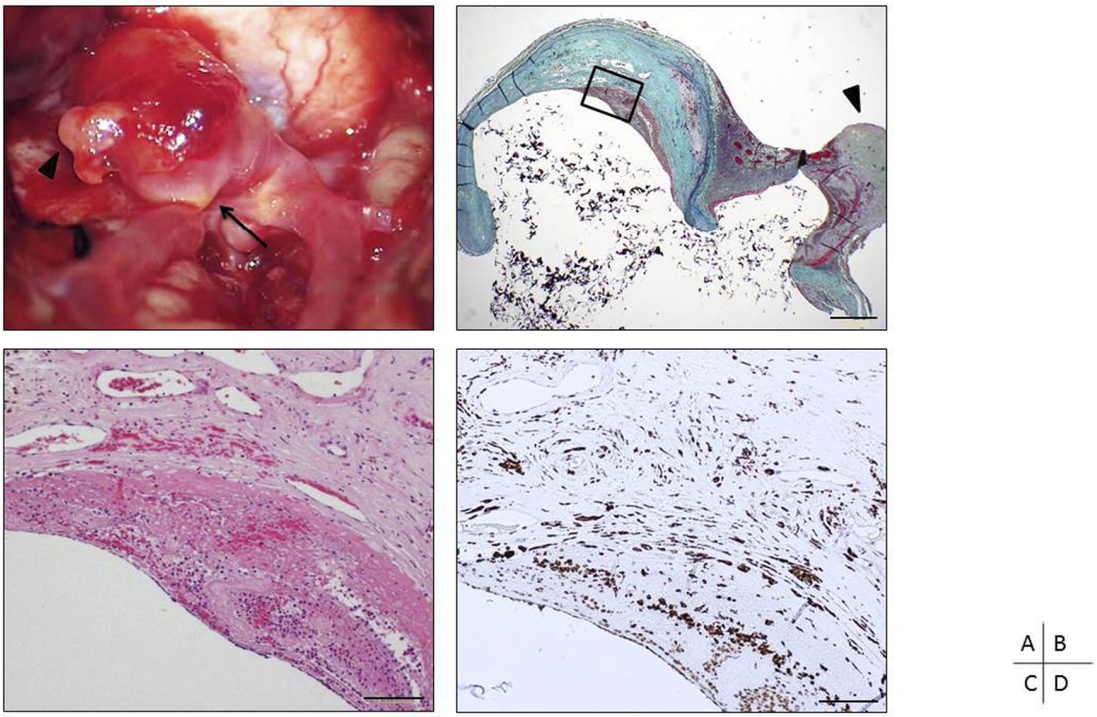

Case No.	Age	Sex	Presentation	Location	Size (mm)
1	67	M	SAH	Lt.MCA	6
2	46	M	SAH	A-com	7
3	61	M	SAH	Rt. dACA	7
4	68	F	SAH	Lt.ICA	4
5	74	F	SAH	Rt.MCA	5
6	47	F	SAH	Rt.ICA	22
7	70	F	SAH	Rt.MCA	5
8	60	F	SAH	Lt.MCA	8
9	56	M	SAH	A-com	3
10	77	M	SAH	A-com	5
11	68	M	SAH	A-com	6
12	74	F	SAH	Rt.MCA	5
13	54	M	SAH	A-com	4
14	53	M	SAH	Rt.MCA	5
15	55	M	SAH	A-com	5
16	61	F	SAH	A-com	7
17	79	F	SAH	Lt.ICA	10
18	66	F	SAH	Rt.MCA	9
19	61	F	SAH	Rt.MCA	8
20	56	F	SAH	Lt.ICA	10
21	78	F	SAH	A-com	5
22	69	F	SAH	Lt.ACA	4
23	58	F	SAH	A-com	7
24	57	M	SAH	Lt.ICA	3
25	76	F	SAH	Rt.ICA	8
26	80	F	SAH	Lt.MCA	12
27	56	F	SAH	A-com	10
28	51	F	SAH	Lt.ICA	3
29	53	M	Incidental	A-com	6
30	59	F	Incidental	Rt.ICA	4
31	70	M	Incidental	A-com	4
32	54	F	Incidental	Rt.MCA	5
33	60	F	Incidental	Rt.ICA	17
34	61	M	Incidental	A-com	4
35	74	M	Incidental	Rt.MCA	5
36	56	F	Incidental	Rt.MCA	5
37	76	F	Incidental	A-com	5
38	54	M	Incidental	A-com	5
39	64	M	Incidental	Lt.ICA	5
40	75	M	Incidental	A-com	11

Table 1

Review of the aneurysms in this study
SAH; subarachnoid hemorrage, MCA; middle cerebral artery, A-com; anterior comunicating artery
dACA; distal anterior cerebral artery, ICA; internal cerebral artery

	Total	Ruptured	Unruptured	univariate P(<0.1)		multivariate P	
Number of patients	40	28	12				
Age mean in y±SD	63.1±9.5	63.2±9.6	63.0±8.7	0.96			
Male/Female	17/23	10/18	7/5	0.18			
Size mean in mm±SD	6.7±3.8	6.9±3.7	6.3±3.8	0.63			
Location (ICA-MCA-ACA)	10-12-18	7-9-12	3-3-6	0.98			
Multiple aneurysms	8 (20%)	4 (14.3%)	4 (33.3%)	0.17			
History of hypertension	22 (55%)	16 (57.1%)	6 (50.0%)	0.68			
Smoking	12 (30;%)	9 (32.1 %)	3 (25%)	0.65			
Hyperlipidemia	16 (40%)	13 (46.4%)	3 (25%)	0.21			
statin	6 (15%)	5 (17.9%)	1 (8.3%)	0.44			
Fragmented Internal elastic lamina	39 (97.5%)	28 (100%)	11 (91.7%)	0.12			
Myointimal hyperplasia	28 (70%)	18 (64.3%)	10 (83.3%)	0.23			
Thining of wall	39 (97.5%)	28 (100%)	11 (91.7%)	0.12			
Subintimal fibrin deposition	28 (70.0%)	26 (92.9%)	2 (16.7%)	<0.001	*	0.015	*
Organized laminar thrombosis	9 (22.5%)	5 (17.9%)	1 (8.3%)	0.44			
Organized intramural hemorrhage	22 (55.0%)	19 (67.9%)	3 (25%)	0.013	*	0.31	
Neovascularization in the wall	21 (52.5%)	19 (67.9%)	2 (16.7%)	0.003	*	0.38	
Chronic inflammation	32 (80.0%)	28 (100%)	4 (33.3%)	<0.001	*	0.84	
The number of CD68 positive cells	51.7±38.8	70.2±29.5	8.6±17.6	<0.001	*		
(Mild chronic inflammation)	7 (17.5%)	4 (14.3%)	3 (25.0%)	0.41			
(Severe chronic inflammation)	25 (62.5%)	24 (85.7%)	1 (8.3%)	<0.001	*	0.019	*

Table 2

Review of the aneurysms in this study

SD indicates standard deviation

MCA; middle cerebral artery, ACA; anterior cerebral artery, ICA; internal cerebral artery